Università degli Studi di Bari

PhD course in Physics – XXXIV cycle

Study of the electro-thermal properties and acoustic coupling of quartz tuning forks

Tutors: Prof. Vincenzo Spagnolo, Dott. Pietro Patimisco
PhD candidate: Stefano Dello Russo

First year PhD report

Introduction

Quartz-Enhanced Photoacoustic Spectroscopy (QEPAS) has been demonstrated as one of the most selective, sensitive, compact, robust and low-cost technique for trace gas optical detection. In QEPAS, a high quality factor quartz tuning fork (QTF) is used as a sharp resonator to detect acoustic waves generated by the non-radiative relaxation of the target gas absorbing radiation. The acoustic waves deflect prongs and an electric signal is generated by exploiting the quartz piezoelectricity. QEPAS does not require bulky optics: a lens is used to focus the laser beam between the two prongs of the QTF. In contrast to other optical detection techniques, QEPAS does not require any optical detector since the QTF itself acts as a detector. The QTF is typically coupled with a pair of tubes, acting as an organ pipe resonator to probe the sound wave. The acoustic detection module composed of the QTF and micro-resonator tubes constitutes the QEPAS spectrophone, which is the core of any QEPAS sensor.
During my first year, a new set of custom QTFs with optimized geometry for QEPAS sensing has been designed, fabricated and tested. Once resonance properties are measured, the investigated QTF samples were implemented in a QEPAS setup to test their photoacoustic response. The QTF providing the best performance in terms of signal-to-noise ratio (SNR) was acoustically coupled with a dual-tube micro-resonator system. A theoretical model has been developed to predict both the optimal internal diameter and length of the tubes of a QEPAS spectrophone as a function of the QTF prongs geometry and spacing between them. With this set of QTFs, an investigation of the photoacoustic response as a function of the resonance frequency has been performed, spanning from 3 kHz to 45 kHz. This study allowed to measure the effective non-radiative relaxation rate of target molecules in a gas matrix. Finally, custom QTFs have been employed in a photoacoustic sensor exploiting interferometric readout (rather than conventional piezoelectric readout) of the mechanical deformation of prongs. Results showed that one readout can be enhanced with respect to the other one by properly selecting the prong geometry.

Quartz tuning forks with optimized geometries for QEPAS

Since its introduction in 2002, standard low-cost quartz tuning forks (QTFs) with resonance frequencies at 32.7 kHz have been typically employed in QEPAS sensors. Starting in 2013, custom QTFs have been realized in QEPAS sensors following the following two guidelines:

- reduction of the QTF fundamental resonance frequency, for an efficient sound wave generation when slow relaxing gases are targeted
- increase the prongs spacing in order to facilitate the optical alignments and minimize the photo-thermal noise level.

The straightforward approach to design QTFs optimized for QEPAS sensing is to reduce the resonance frequency while keeping high the quality factor. Based on the results obtained with the 1st generation of custom QTF in 2013, a MATLAB-based software to relate the QTF quality factor and its resonance frequency to its prongs geometries

has been developed. For each fixed prong geometry (T-prong width, L-prong length), the software calculates the resonance frequency and the related Q-factor, and plots ordered points on the x- (resonance frequencies, *f*) and y- (*Q*-factors) axis of the coordinate plane. By ranging L from 3 mm to 20 mm and T from 0.2 mm to 3.0 mm, while keeping fixed the crystal thickness at w = 0.25 mm value, the calculated ordered points (Q, f) are shown in Fig. 1.

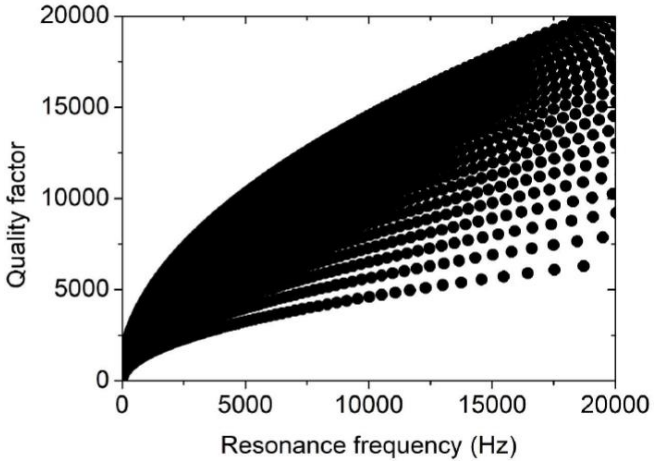

Figure 1. *Q*-factor values plotted as a function of the resonance frequency for different prong lengths and thicknesses of quartz tuning fork of crystal width w = 0.25 mm, at atmospheric pressure.

At f = 16 kHz, an half of the resonance frequency of the standard QTF, L and T values maximizing the quality factor (18,000) are 9.4 mm and 2.0 mm, respectively. Starting with this prong geometry, two QTFs differing only in the prong spacing has been designed: QTF-S08 having a prong spacing of 0.8 mm, and QTF-S15 with a prong spacing of 1.5 mm, in order to make a comparison between them in terms of QEPAS performance and evaluate the influence of the prong spacing on the resonance properties. Starting from QTF-S08, a modified geometry for QTF prongs is proposed, in which the prong thickness T is not constant along the prong axis. The optimal QTF geometry was determined by using COMSOL Multiphysics, evaluating the QTF stress field intensity. This prong geometry will be referred as a T-shaped prong and the fork will be indicated as QTF-S08-T. The sizes of all three QTFs are shown in Fig. 2.

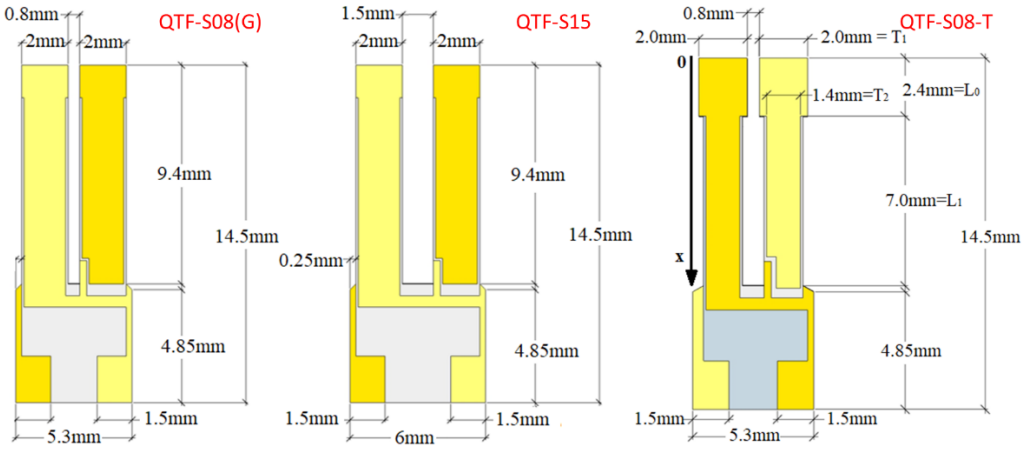

Figure 2. Dimensions of the set of custom QTFs realized.

First, the resonance properties were determined by exciting the fundamental flexural mode with a sinusoidal voltage signal. Then, the investigated QTF samples were implemented in a QEPAS setup to test their photoacoustic response. The QTF-S08-T provided the best performance in terms of signal-to-noise ratio (SNR) and it was acoustically coupled with a couple of tubes in dual-tube on-beam configuration. A study of the SNR enhancement was carried out as a function of the tubes geometrical parameter, namely the internal diameter, the length, and the distance between tubes and QTF. As representative, Figure 3 shows the acquired QEPAS signals as a function of the tubes length when the internal diameter is 1.52 mm and the distance between tubes and QTF is 200 µm.

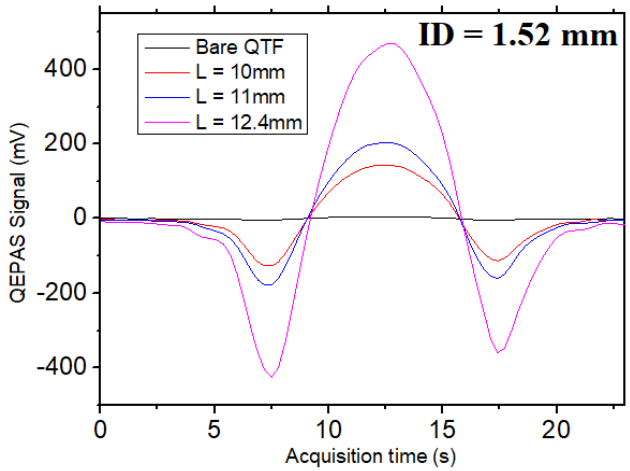

Figure 3. QEPAS signals obtained with micro-resonators of different lengths and tube internal diameter of 1.52 mm.

In the best configuration, a SNR enhancement of 60 times was obtained with respect to the bare QTF, which represents a record value for dual-tube spectrophones in QEPAS systems.

Acoustic coupling between quartz tuning forks and micro-resonator tubes

For a selected QTF, the geometric parameters influencing the sensor performance are the internal diameter (ID) and the length of the two tubes L. The length of the two tubes is correlated with the sound wavelength $\lambda = v_s/f_0$, where v_s is the sound speed in the sample gas mixture. If the gap between the tubes is neglected, each tube forms a half-wave resonator with the QTF placed on the antinode point of the sound field. A sketch of the spectrophone is given in Fig. 4.

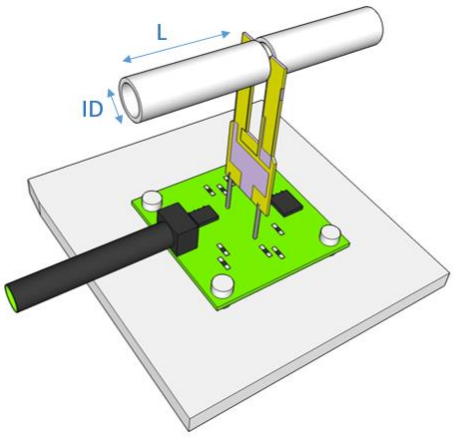

Figure 4. Sketch of QEPAS spectrophone in on-beam dual-tube configuration.

Experimental studies have shown that the optimal tube length is less than $\lambda/2$ and this effect has been ascribed to the interaction between the two resonator tubes and to their acoustic coupling with the QTF, while the choice of the optimal tube internal diameter has been related only to the QTF prongs' spacing. So far, there is no way to predict in advance the best resonator geometrical parameters and they must be determined experimentally. We realized a theoretical model capable of predicting both the optimal internal diameter and length of the tubes of a QEPAS spectrophone as a function of the QTF prongs geometry and spacing. The theoretical model is based on the open-end correction of resonators, the divergence of the sound field exiting one tube, and its acoustic coupling with the other tube.

When a sound wave generated by a source located close to one end of the resonators propagates through a resonator tube, a standing wave vibrational pattern is created within the resonator when multiple reflected waves from the ends of the resonator constructively interfere with the incident wave, in a way that makes specific points along the resonator appear to be standing. If the resonator tube diameter is small compared to the sound wavelength, the excited sound field varies only along the resonator length, resulting in a one-dimensional acoustic field. Hence, a resonator tube can be considered as a one-dimensional acoustic resonator. In this approximation,

a nearly complete reflection of a dominant mode sound wave occurs at the open end of the resonator. Hence, the standing wave pattern's antinodes should correspond to the open ends of micro-resonator. Actually, the antinode of a standing sound wave in a resonator with an open end is located slightly outside the end point, at a distance called the open-end correction (OEC). The OEC can be explained by considering the effect of the air surrounding the resonator on the pressure field inside the tube. The mismatch between the one-dimensional acoustic field inside the resonator and the three-dimensional field radiated by the open end outside the resonator causes the pressure field outside the tube to oscillate with the one inside. Therefore, differing from the free-edge boundary conditions, the air inside the tube is affected by the reaction force from the air outside. As a result, the antinode appears a little away from the end of the tube. The OEC value Δl has been estimated as:

$$\Delta l = \frac{8a}{3\pi} \tag{1}$$

where a is the radius of the acoustic resonator. The OEC should be added to the length of the tube. Thereby, the effective length of the resonators for the dominant mode (n = 1) can be estimated:

$$l = \frac{v_s}{2f_0} - \frac{16a}{3\pi}. \tag{2}$$

Hence, the optimal tube length depends on its radius. To predict the optimal tube radius, a theoretical model developed by Levine and Schwinger in 1948 (Phys. Rev. 1948, 73, 383–406) has been adopted. It is based on the estimation of the power gain function $G(\vartheta, ka)$, i.e. the distribution of the sound emitted by an isotropically radiating point source at an angle ϑ measured from the axis of the resonator. The power gain function depends on the product between the tube internal radius a and the sound wavelength k. Then, the acoustic coupling between two tubes has to be considered. the two tubes can be considered as a 1D single resonator. According to the theoretical model proposed, the optimal distance between the tubes is the one maximizing the sound energy transfer from one tube to the other. Geometrically, the transferred energy corresponds to the energy propagating within the cone having vertex in the center of the open end of one tube and base the outer section of the opposite tube, as shown in Fig. 5.

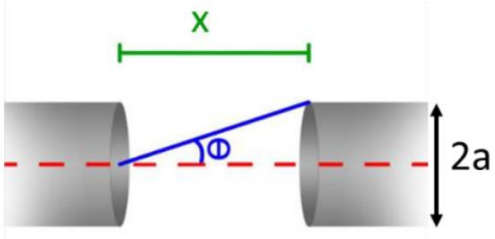

Figure 5. Schematic of two tubes separated by a distance *x*.

With a fixed tube diameter *2a*, the vertex angle of the cone scales with the tube distance x as $\vartheta(x) = tan^{-1}(a/x)$. Hence, the amount of transmitted energy can be estimated by integrating $G(\vartheta, ka)$ from *0* to $\vartheta(x)$. To validate the model, a QEPAS spectrophone composed by a QTF-S15 and micro-resonator tubes having a length of 9.5mm and internal diameter of 1.59 mm has been employed. The experimental results and theoretical data are plotted in Fig. 6 as a function of the distance *x*.

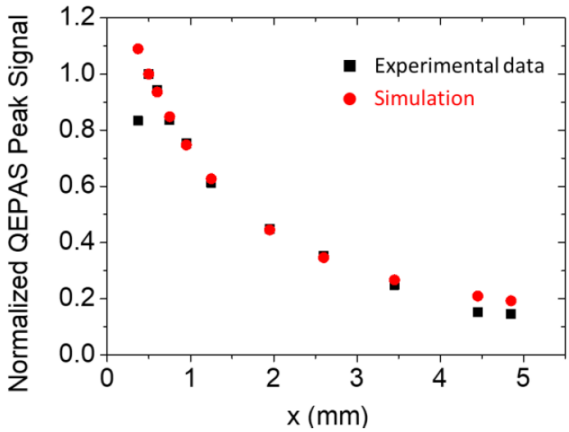

Figure 6. Normalized QEPAS Peak signal as a function of the distance between the two tubes (black squares), together with the theoretical simulation (red dots).

For 550 µm ≤ *x* ≤ 4.8 mm, the theoretical model matched the experimental data, proving that the QTF acted as a perfect probe for the acoustic field intensity measurement in the area between the two tubes. The highest intensity QEPAS signal occurred at *x* = 550 µm, which corresponds to an optimal distance between the QTF surface and the tubes of 150 µm, considering a 250 µm crystal thickness. For a shorter distance, *x* = 400 µm, the QTF signal was reduced. This drop was not predicted by the theoretical model but can be explained by considering that when tubes are too close to the QTF, they generate a damping of QTF vibrations, causing an overall quality factor decreasing that negatively affects the QTF signal. At distances larger than 5 mm, the sound energy transfer between the tubes was highly reduced; therefore, these distances are not feasible for QEPAS sensing. Once validated, the theoretical model has been used to predict the optimal tube radius that maximizes the QTF signal. Placing both tubes at a distance of 150 µm away from the QTF, the vertex angle of the cone will scale according to $\vartheta(a) = tan^{-1}(a/0.55)$ as a function of the tube radius *a* (in millimeters). However, if the prong spacing becomes lower than the tube diameter, part of the sound field exiting from the tube will be shielded by the QTF surface. As a consequence, the effective angle ϑ will become $s/0.55$, for all $a>s/2$. The amount of energy transfer can be estimated by integrating $G(\vartheta, ka)$ from *0* to $\vartheta(a)$. For a standard 32.7-kHz QTF, the model predicted optimal tube diameters in the range 400–800 µm, in agreement with the values experimentally found in previous studies. Using QTF-S15 with a prong spacing of 1.5 mm, the theoretical optimal tube diameter falls in the range 1.4 mm ≤ a ≤ 1.8 mm, in excellent agreement with the experimental value (1.4 - 1.6 mm). Once the optimal internal diameter is determined, the optimal tube length can be predicted. In Table 1, the tube lengths predicted using Eq. 2 were compared with those experimentally found to maximize the QTF signal (L_{exp}).

QTF	Prong Spacing (mm)	ID (mm)	λ/2 (mm)	L_{th} (mm)	L_{exp} (mm)	QEPAS SNR Enhancement
Standard	0.3	0.6	5.25	4.73	4.4	30
QTF#2	0.8	1.3	23.89	22.79	23	40
QTF#4	1	1.52	6.76	5.47	5.3	15
QTF#T1	0.8	1.59	13.79	12.43	12.4	60

Table 1. Best geometry parameters of dual-tube spectrophones realized for four di_erent QTFs operating at different frequencies: the prongs' spacing, the internal diameter of the tube (ID), the sound half wavelength (λ/2), and the theoretical (L_{th}) and experimental (L_{exp}) optimal tube lengths.

From this comparison, it is evident that the OEC predicts the optimal tube length well with an uncertainty of less than 10%.

Measurement of gas relaxation rate in a matrix by using QEPAS technique

The QEPAS technique can be used to measure the non-radiative relaxation rate of a gas target in a matrix. The QEPAS signal *S* can be expressed as a function of:

$$S(p, f, p_0\tau_0) = K_{st} P_L C_{gas} Q(p) \varepsilon(p, f, p_0\tau_0) \quad (3)$$

where K_{st} is a QTF constant, P_L is laser optical power, C_{gas} is target gas contentration. The parameter ε is the radiation-to-sound conversion efficiency which depends on pressure p, resonance frequency f and acoustic relaxation rates, $p_0\tau_0$, of the excited molecules when are immersed in a matrix. ε(P) depends on vibration-translation (V-T) energy transfer and it is related to gas matrix properties. It can play a fundamental role in the estimation of the gas target concentration. It has been shown that the use of standard QTFs (32.7 kHz) limits the ultimate detection capability of QEPAS when slow-relaxing gases species, like NO and CO, has to be detected. To overcome this limitation, relaxation promoters (typically H_2O or SF_6) are added to the gas sample mixture to enhance the detection sensitivity. In this case, the QEPAS signal depends also on the concentration of relaxation promoter that it has been measured for a correct estimation of the gas target concentration. This can be avoided if the acoustic relaxation rates can be measured. ε(P) as a function of the pressure is given by:

$$\varepsilon(p) = \frac{1}{\sqrt{1+\frac{(2\pi f p_0\tau_0)^2}{p^2}}} \quad (4)$$

where f is the QTF resonance frequency. ε(P) depends on the product between resonance frequency and relaxation rate. Both ε(P) and Q(P) are a function of gas pressure. With a fixed gas target concentration, the trend of QEPAS signal and quality factor as a function of gas matrix pressure for QTF having a resonance frequency of 3.4 kHz is reported in Fig. 7.

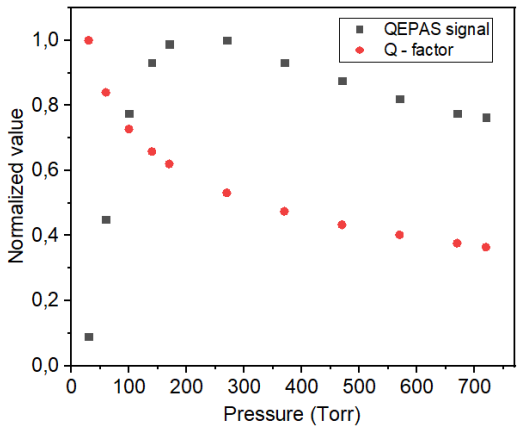

Figure 7. Normalized QEPAS methane signal and quality factor obtained with a custom QTF operating in the fundamental mode (3.44 kHz) on a mixture of 1% CH_4, 0.15% H_2O and 98.85% N_2.

Starting from atmospheric pressure till 250 torr, the QEPAS signal increases as the pressure decreases, benefiting from the increase of the quality factor (see Eq. 3). Conversely, when P < 250 torr, the QEPAS signal decreases even if the QTF quality factor rapidly increases. This can be explained in the following way: when the pressure decreases, the matrix molecule density is reduced as well as the collision probability with neighbored partners, thus in turn reducing the radiation-to-sound conversion efficiency. Hence, the trend of S(P)/Q(P), as a function of the matrix pressure should vary for different resonance frequencies, at a fixed gas concentration. With a certified mixture of 1% CH_4, 0.15% H_2O and 98.85% N_2, the ratio S(P)/Q(P) have been measured in the pressure range 20 – 760 torr, by using 4 QTFs with following resonance frequencies: 3.44 kHz (QTF#1), 9.78 kHz (QTF#2), 15.73 kHz (QTF#3) and 21.43 kHz (QTF#4).

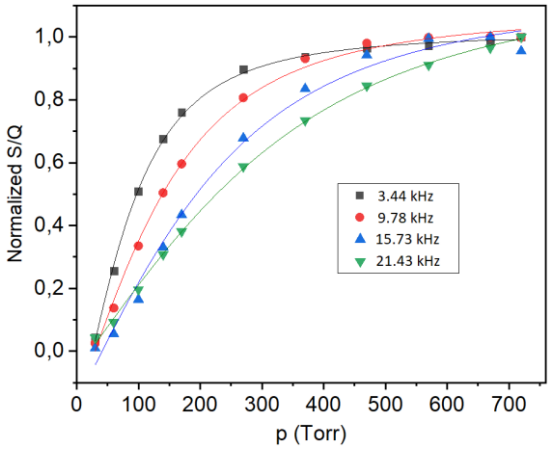

Figure 8. Radiation-to-sound conversion efficiency function for four different resonance frequencies of V-T relaxation of CH_4 on a mixture of 1% CH_4, 0.15% H_2O and 98.85% N_2. The points represent the experimental values normalized to the maximum value, obtained by dividing the acquired QEPAS signal and quality factor for each pressure. The lines represent the fit performed.

The results are shown in Fig. 8. For each resonance frequency, data are normalized to the highest value. In this way, S(P)/Q(P) follows the trend of ε(P) and experimental data can be fitted by using Eq. 4. From the fits, the parameter $A = 2\pi f p_0 \tau_0$, can be retrieved in order to estimate the effective relaxation rate of CH_4. The parameter A plotted as a function of the resonance frequency is shown in Fig. 9.

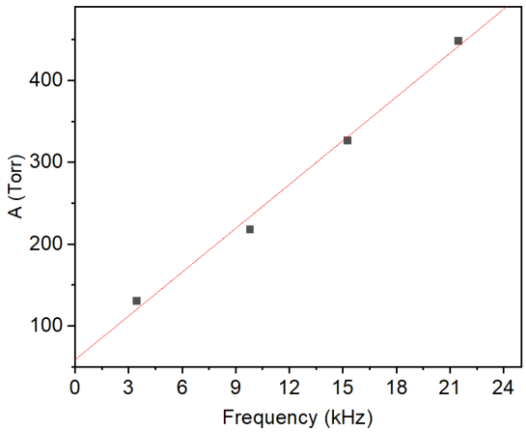

Figure 9. Black dots: values of parameter *A* obtained by fitting on the experimental curves of the radiation-to-sound conversion efficiency. Red line: linear fitting performed on the values of parameter *A* obtained.

The estimated relaxation time retrieved by the slop of the best linear fit is τ_{MEAS}=(3.2±0.1) msTorr, in excellent agreement with the estimation obtained with ultrasonic velocity dispersion and classic photoacoustic technique (τ_{EST}=3.3msTorr, ref. [1,2]).

Interferometric PAS with custom QTFs

In standard QEPAS the deformation of the QTF prongs due to the impact of the generated acoustic wave induces a charge accumulation. This piezoelectric charge is subsequently collected by a gold pattern deposited on the QTF and transformed into a voltage signal by means of a transimpedance amplifier. However, piezoelectric readout cannot be used in applications where high electromagnetic fields would affect the electric signal or for explosive detection, where electrical sparks may trigger gas deflagration. To overcome these limitations, deflections of the prongs in QEPAS can be measured by optical readout methods based on a laser interferometer, which adapts well to multiplexing. Laser interferometers have demonstrated to be able to measure displacements with accuracies to the level of the picometer. Compact interferometric systems integrating near-infrared diode lasers and photodetectors are commercially available. If optical readout is adopted in a QEPAS sensor, no electrical contacts are needed for the acoustic detection module.

The signals obtained by using only one readout method and by using both approaches simultaneously showed the same spectral intensity and profile. This result confirms that there is no cross-talking between the two readout methods and, therefore, that the use of one does not affect the performance of the other one. Fig. 10 shows the piezoelectric and the optical signal for bare QTF-T08 acquired while the laser wavelength was scanned across two water absorption lines.

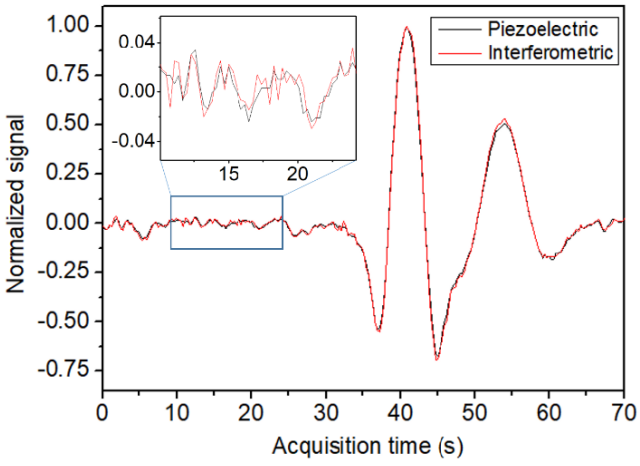

Figure 10. Piezoelectric (black curve) and interferometric (red curve) PAS signals normalized and superimposed, measured using the T-QTF. In the inset is show an enlarged view of the noise fluctuations.

By coupling the QTF-T08 with micro-resonator tubes, an SNR enhancement of a factor of 16 was obtained for the piezoelectric readout, while for the interferometric readout an enhancement of about 13 was obtained. This can be ascribed to the fact that T-shaped QTF was properly designed to offer high QEPAS performance for piezoelectric readout. In order to confirm the hypothesis that by properly designing the prongs geometry it could be possible to selectively enhance the sensitivity of the piezoelectric or interferometric readout, the T-shaped QTF has been replaced with a QTF#1. The SNR obtained with the interferometric technique results to be about 50% higher than the piezoelectric one. A direct comparison between QTF-T08 and QTF#1 when optical readout is used can be done by estimating the vibration amplitude of both QTFs, given by:

$$a = \sqrt{\frac{QVI}{2\pi f k}} \tag{5}$$

where *Q* is the QTF Q-factor, *f* its resonance frequency, *V* is the voltage across the QTF, *I* the generated piezo-current and *k* the QTF spring constant. The latter was estimated by using a finite element analysis based on COMSOL Multiphysics, while *Q,V,I* and *f* values were measured via electrical characterization. The ratio between the vibration amplitude for the QTFs results $a_{QTF\#1}/\ a_{QTF\text{-}T08}$ = 2.6, comparable with the ratio between peak interferometric readout signals $S_{QTF\#1}/\ S_{QTF\text{-}T08}$= 2.13. Hence, the larger the vibration amplitude, the higher the optical readout signal. This proves that the QTF geometry could be optimized when interferometric measurement systems are to be adopted. The SNRs obtained with the two techniques and the two QTF analyzed are summarized in Table 2.

	QTF-T08	**QTF#1**
Piezoelectric readout (SNR)	**84**	23
Interferometric readout (SNR)	60	**35**

Table 2. Signal-to-noise ratios (SNRs) measured for I-QTF and T-QTF, when piezoelectric or interferometric readouts are selected.

Despite the highest PAS interferometric signal has been measured with the QTF#1, the highest interferometric SNR (60) has been achieved when using QTF-T08. This is due to the *1/f* dependence of the noise level, demonstrating that the optical readout is sensitive to the flicker noise of the acoustic source. Thus, even if the vibration amplitude is the figure of merit to be optimized to enhance the optical readout signal, moving to lower frequency negatively affects the noise level. For the piezoelectric readout, the ultimate noise level is dominated by the thermal noise of the QTF and the electronic noise of the transimpedance amplifier, which usually scales linearly with the resonance frequency.

References

[1] H. E. Bass and H.-J. Bauer, Kinetic Model for Thermal Blooming in the Atmosphere, Appl. Opt. 12, 1506 (1973).
[2] S. Schilt, J.-Ph. Besson, L. Thévenaz, Near-infrared laser photoacoustic detection of methane: the impact of molecular relaxation J. Phys., IV 125, 7 (2005)

List of attended courses

- Promozione della ricerca scientifica (Prof. De Gennaro)
- How to prepare a technical speech in English (Prof. White)
- Programming with Python for Data Science (Prof. Diacono)
- Atom-photon interactions (Prof. Pepe)
- Optical sensors and spectroscopic techniques (Prof. Patimisco)
- Applications of MATLAB (Prof. Dotoli)
- Introduction to C++ programming (Prof. Cafagna)

List of publications

- P. Patimisco, A. Sampaolo, M. Giglio, **S. Dello Russo**, V. Mackowiak, H. Rossmadl, A. Cable, F.K. Tittel, V. Spagnolo, "Tuning forks with optimized geometries for quartz-enhanced photoacoustic spectroscopy", Opt. Express **2019**, 27, 1401–1415.
- **S. Dello Russo**, M. Giglio, A. Sampaolo, P. Patimisco, G. Menduni, H. Wu, L. Dong, V.M.N Passaro, V. Spagnolo, "Acoustic Coupling between Resonator Tubes in Quartz-Enhanced Photoacoustic Spectrophones Employing a Large Prong Spacing Tuning Fork", Sensors **2019**, 19(19), 4109.
- **S. Dello Russo**, S. Zhou, A. Zifarelli, P. Patimisco, A. Sampaolo, M. Giglio, D. Iannuzzi, V. Spagnolo, "Photoacoustic spectroscopy for gas sensing: a comparison between piezoelectric and interferometric readout in custom quartz tuning forks", Photoacoustics, **submitted**.

Conference proceedings

- **S. Dello Russo**, P. Patimisco, A. Sampaolo, M. Giglio, G. Menduni, A. Elefante, V.M.N. Passaro, F.K. Tittel, V. Spagnolo, "Measurement of non-radiative gas molecules relaxation rates by using quartz-enhanced photoacoustic spectroscopy", Proc. SPIE, Quantum Sensing and Nano Electronics and Photonics XVII, **2020**, **accepted**.
- P. Patimisco, S. Zhou, **S. Dello Russo**, A. Zifarelli, A. Sampaolo, M. Giglio, H. Rossmadl, V. Mackowiak, A. Cable, D. Iannuzzi, V. Spagnolo, "Comparison between interferometric and piezoelectric readout of tuning fork vibrations in quartz-enhanced photoacoustic spectroscopy", Proc. SPIE, Quantum Sensing and Nano Electronics and Photonics XVII, **2020**, **accepted**.
- P. Patimisco, A. Sampaolo, M.Giglio, **S. Dello Russo**, A. Zifarelli, G. Menduni, F. Sgobba, A. Elefante, H. Wu, L. Dong, F.K. Tittel, V. Spagnolo, "Trace Gas Detection with Quartz-enhanced Photoacoustic Spectroscopy for Real World Applications" – Proceedings of PIERS **2019** in Rome.
- P. Patimisco, A. Sampaolo, M. Giglio, **S. Dello Russo**, A. Elefante, G. Menduni, V.M.N. Passaro, H. Rossmadl, V. Mackowiak, B. Gross, A. Cable, F. K. Tittel, and V. Spagnolo "New generation of tuning forks for quartz-enhanced photoacoustic spectroscopy", Proc. SPIE 10926, Quantum Sensing and Nano Electronics and Photonics XVI, 109260D, **2019**.
- P. Patimisco, V. Spagnolo, A. Sampaolo, **S. Dello Russo**, M. Giglio, L. Dong, F.K. Tittel, "Improvements In Quartz-Enhanced Photoacoustic Spectroscopy By Employing Optimized Tuning Forks", Proceedings of ICMAT **2019**, 190653.